Materials Research, Vol. 5, No. 3, 287-293, 2002.

Carbonation-Related Microstructural Changes in Long-Term Durability Concrete

Cláudio A. Rigo da Silva[a]*, *Rubens J. Pedrosa Reis*[b], *Fernando Soares Lameiras*[c] *and Wander Luiz Vasconcelos*[d]

[a] *Dep. of Materials Engineering and Civil Construction, Federal University of Minas Gerais, Rua Espírito Santo, 35, 30160-030 Belo Horizonte - MG, Brazil*
[b] *Dep. of Civil Engineering, FUMEC, Rua Cobre, 200 30310-190 Belo Horizonte - MG, Brazil*
[c] *Nuclear Technology Development Center (CNEN/CDTN) Av. Mário Werneck, s/n – Cidade Universitária, 31270-901 Belo Horizonte - MG, Brazil*
[d] *Dep. of Metallurgical and Materials Engineering, Federal University of Minas Gerais Rua Espírito Santo, 35, 2nd fl., 30160-030 Belo Horizonte - MG, Brazil*

Received: September 27, 2001; Revised: July 10, 2002

This paper discusses the effects of carbonation on the microstructure of Portland cement concrete for long-term durability applications. A class C40 concrete (characteristic compression strength between 40 MPa and 44 MPa on the 28th day, according to Brazilian standard NBR 8953) was chosen for the experimental study of the carbonation effects, from which test samples were molded for accelerated test under a 100%-CO_2 atmosphere after physical and mechanical characterization. It was observed that carbonation provoked a reduction of 5% to 12% of the concrete open porosity accessible to water. Flexural strength values obtained after the carbonation tests revealed a decrease of 12% and 25% in relation to the values obtained before tests on the 28th and 91st days, respectively.

Keywords: *concrete, carbonation, microstructure, long-term durability*

1. Introduction

The increasing concern for reinforced concrete structure durability is justified in many ways: concrete is cheap and relatively easy to obtain anywhere in the world, in comparison to other building materials; the deterioration of concrete structures causes great losses to the world economy; reinforced concrete deterioration mechanisms can be better understood and prevented; this is an important field of study which started to be better explored 20 years ago, enabling the production of good concrete with specific physical properties, with the rational use of cement and the addition of minerals, many a time from industrial wastes. In contrast, the concern with world sustainable development has lead to studies and economic and ecological decisions aiming to optimize the use of natural resources in the manufacture of the several types of cement, since cement world consumption has increased unceasingly[1].

In the recent years, it has been observed in many parts of the world that one of the major causes of the deterioration of reinforced concrete structures is reinforcement corrosion[2,3]. The durability of the reinforced concrete structures depends basically on the microstructural properties of the concrete, since the integrity of the steel bars is a direct function of the capacity of the concrete to serve as a barrier to aggressive agents. This is the reason why one comes across truly discrepant cases side by side: a Roman Pantheon which has lasted more than 2000 years built with simple concrete of extremely low strength (around 10 MPa) and the modern concrete structures with twice as much strength and which is in critical state of deterioration little older than ten years. The presence of the reinforcement without sufficient protection is responsible for this discrepancy. Concrete carbonation is directly related to reinforce-

*e-mail: claudio@demc.ufmg.br

ment corrosion: it creates a chemical unbalance and lowers the pH of concrete, which facilitates reinforcement depassivation, and also enhances adverse chloride and sulfide reactions.

The action of CO_2 progresses from the outside to inside in the form of a carbonation front, although some authors point out that the penetration of carbon dioxide does not necessarily produce a well defined front, and that punctual advances may occur[4] Whatever the case, it is necessary to slow down this advance to the most to obtain durable reinforced concrete structures. Therefore, for the layer of concrete on the reinforcement (coating) to be an effective protection it is necessary that it present other characteristics besides appropriate thickness: suitable microstructure density, low porosity and connectivity between the pores, which leads to low permeability[5]. Such characteristics can be obtained from a concrete which presents low hydration heat, small water/cement ratio, low exudation and plastic shrinkage[2].

Most chemical reactions among the aggressive elements and the concrete components occur in the water contained in the pores. Therefore, for an adequate approach of the durability of reinforced concrete structures, it is important to know the material pore structure, the degree of saturation of these pores, that is, the volumetric fraction of the pores of the material that contain gaseous and aqueous phases, and the evolution of the concentration of the cement constituents which can be attacked with time[6,7].

In the case of carbonation, air contains CO_2, which reacts with cement hydrated compounds in the presence of moisture. The carbonation reaction itself is not hazardous to cement, except for the increase in shrinkage, which can occur under certain conditions. The concern about carbonation increases when one considers reinforced concrete structures, because a reduction in the pH of the water in the pores of concrete from 12.6-13.5 to values around 9 provokes the depassivation of the reinforcements, exposing them to corrosion[8-13].

2. Research Significance

The current work presents the results of a study, which aims to clarify the effects of carbonation reaction on the microstructure of concrete. The experimental strategy used was the microstructural characterization of class C40 concrete, before and after accelerated carbonation tests. The behavior of the material was evaluated by means of the mechanical properties of tensile, by flexural and splitting tests and axial compression. The microstructural parameters considered were porosity, measured by means of two different methods; carbonation depth, given by the variation of the material pH (phenolphthalein); and the identification of carbonates by means of electronic scanning microscopy. The correlation between the microstructure and the properties allowed the evaluation of the action of CO_2 in concrete.

3. Experimental Program

The concrete selected, class C40, was made with cement CPII E 32 (composite cement added with 25% slag and 10% limestone), washed sand, coarse gneiss aggregate with maximum 25 mm diameter, and accelerating water-reducing admixture. Tables 1 and 2 show the main characteristics of the aggregates and the dosage used. Twenty-eight cylindrical test samples (ϕ 15 × 30 cm) and 14 prismatic test samples (15 × 15 × 75 cm) were cast according to Brazilian standard NBR 5738. Table 3 presents the results of the mechanical tests of axial compression, tensile and

Table 1. Characteristics of Main Aggregates.

Characteristics	Fine Aggregate	Coarse Aggregate
Maximum Diameter (mm)	2.4	25
Fineness Modulus	2.62	7.02
Content of Powder Coating Materials (%)	0.35	0.13
Dry Unitary Weight (kg/m^3)	1419	1409
Wet Unitary Weight (kg/m^3)	1135	—
Real Specific Weight (kg/m^3)	2604	2682
Clay Lumps Content (%)	0.021	—

Table 2. Typical Mix Proportions for Strength Group C40 Concrete.

Materials	Mix Proportions
Cement (kg/m^3)	430
Fine Aggregates (kg/m^3)	605
Coarse Aggregates (kg/m^3)	1104
Superplasticizer REAX 3000 A (kg/m^3)	2.2
Water (l/m^3)	178.94
A/C ratio	0.42
Air Content (%)	4.1
Slump test (mm)	85

Table 3. Mechanical Properties of C40 Concrete.

Age (days)	Tensile Strength (MPa)	Flexural Strength (MPa)	Compressive Strength (MPa)
3	2.2	4.7	29.5
7	2.8	5.0	33.8
28	3.9	5.9	41.8
91	4.7	6.9	46.6

flexural strength up to the age of 91 days.

A special chamber was prepared for carbonation tests, which allowed submitting the test samples to a controlled atmosphere with relative moisture and temperature coinciding with those of the laboratory (around 60% and 20 °C, respectively). A composition of 100% CO_2 was chosen for the chamber atmosphere in agreement with experiments reported in literature[14,15].

4. Test Results

In the first stage, two prismatic test samples – P40CC and P40DC – were submitted to the CO_2 atmosphere for 28 days. After the tests, flexural strength and depth of carbonation by phenolphthalein in the rupture section were measured. These data are presented in Table 4.

Open porosity of the concrete samples was measured according to the RILEM[16] procedures to obtain the porosity accessible to water. Eight cubic samples (two of each test sample) with approximately 10 cm corners were cut from four cylindrical test samples (ϕ 15 × 30 cm) – C40EC, C40FC, C40GC and C40HC. The advantage of this procedure is obtaining a concrete sample, which was not carbonated in the practice. These samples were initially protected from air with a plastic film, and later kept in oven at 65 °C for a period equal or superior to three weeks until the mass remained constant. This mass was called dry mass. After reaching this condition, the sample was submitted to vacuum for 24 h, and later kept submersed in water for another 24 h for hydrostatic and saturated mass measurements. The following parameters, presented in Table 6, were calculated based on these values[17]:

a) Porosity: ratio between the volume of pores accessible to water and the apparent volume of the sample;
b) Real volumetric mass (Dr): volumetric mass of the impermeable material, i.e., the ratio between dry sample mass and impermeable material volume;
c) Apparent volumetric mass (Da): ration between dry sample mass and its apparent volume.

Of the eight samples mentioned above, six were submitted to a 100%-CO_2 atmosphere for 25 days. The two remaining samples – C40EC2 and C40FC1 – were kept in air for control. After the accelerated carbonation test period, the RILEM procedure was repeated to obtain the porosity accessible to water for the eight samples. The results are also shown in Table 6.

From the carbonated samples, mortar involving the thick aggregate portions was taken for mercury porosimetry using an AutoPore III 9420 (Micromeritics) capable of reaching pressures in the order of 414 MPa. The mortar portions were taken near the sample surface, and an A index was added to the sample name, and from the central region of the sample, added with a B index. Figure 2 shows the mercury intrusion curves for the two carbonated samples (C40EC1 and C40GC2) and of a control sample (C40EC2). The parameters obtained from the mercury porosimetry are presented in Table 7.

Figures 3 and 4 show aspects of the microstructure of the concrete analyzed. The hydration products were formed normally and the microstructure was compact and with few voids (Fig. 3). Some carbonates were identified as light particles and with smooth surface (Fig. 4).

Table 4. Flexural Strength and Depth of Carbonation.

Specimen	Flexural Strength (MPa)	Depth of Carbonation (mm)	
P40CC	5.2	Below Surface, without air contact:	0
		Lateral Faces:	1-3
		Surface with air contact:	8-10
P40DC	5.1	Below Surface, without air contact:	0
		Lateral Faces:	2
		Surface with air contact:	2-3

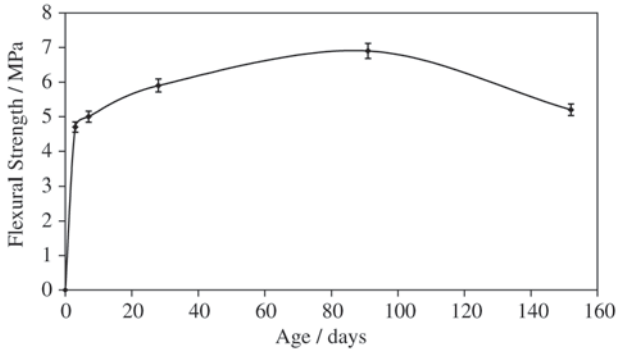

Figure 1. Flexural Strength of C40 Concrete.

Table 5. Mechanical Properties of Concrete After Carbonation Test.

Specimen	Depth of Carbonation (mm)	Load at Rupture in Axial Compression Test (ton)
C40EC1	8 – 15	57
C40EC2	1	32
C40FC1	1	35
C40FC2	8 – 15	52.5
C40GC1	8 – 15	54.5
C40GC2	8 – 15	49.2
C40HC1	8 – 15	49
C40HC2	8 – 15	43

Table 6. Porosity Accessible to Water, Before and After Carbonation Test.

Specimen	Before Carbonation Test			After Carbonation Test		
	P (%)	Dr (kg/m^3)	Da (kg/m^3)	P (%)	Dr (kg/m^3)	Da (kg/m^3)
C40EC1	9.0	2781.1	2531.3	7.9	2603.4	2398.5
C40EC2	8.6	2790.4	2551.4	8.1	2576.2	2368.5
C40FC1	8.8	2572.7	2345.9	9.7	2586.9	2336.5
C40FC2	8.6	2819.7	2577.9	7.9	2607.3	2400.3
C40GC1	7.5	2564.4	2373.1	7.3	2601.9	2412.1
C40GC2	8.4	2778.3	2543.5	7.8	2598.9	2396.0
C40HC1	8.4	2790.0	2554.8	7.8	2610.1	2407.2
C40HC2	9.4	2829.8	2564.9	7.6	2606.0	2407.1

Table 7. Parameters Obtained with Mercury Intrusion Porosimetry.

Specimen	Open Porosity (%)	Pore Surface Area (m^2/g)	Retention Factor R (%)	Threshold Diameter (μm)	dV/dD at Final Intrusion (m^2/g)	D_m (μm)
C40EC1A	13.0	11.6	77.5	0.0144	0.9081	0.1238
C40EC1B	11.8	7.6	75.2	0.0144	1.579	0.2745
C40EC2A	13.4	4.8	54.8	0.1443	0.776	0.2123
C40EC2B	12.5	4.2	56.5	0.1441	0.9793	0.2695
C40GC2A	8.9	4.5	71.9	0.0144	0.000	0.1322
C40GC2B	9.2	4.1	71.2	0.027	1.357	0.2767

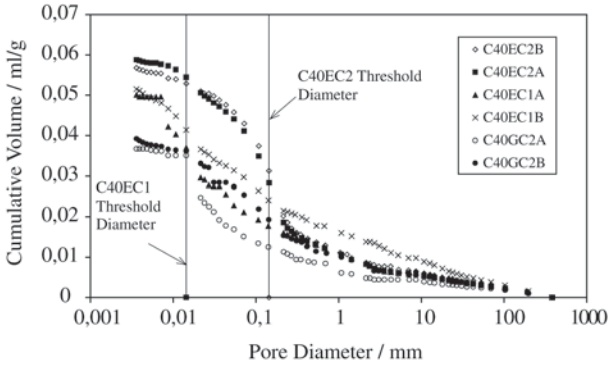

Figure 2. Mercury Intrusion Curves of Carbonated and Control Samples.

5. Discussion

The carbonated concrete seems to present diminished flexural strength. This can be observed in Fig. 1 and also in the comparison of Tables 3 and 4. The values of flexural strength decreased by 12% and 25% in relation to the values in the previous 28 and 91 days, respectively. At least one of the prismatic test samples (P40CC) had larger values of carbonation depth on the surface, which means that the face was not protected by the metallic mold used in casting the test sample. It seems reasonable that the unprotected face of the test sample would be more porous than the others.

The cubic carbonated samples stood loads significantly higher (22% to 78% higher) than the control sample up to rupture did, as shown in Table 5. These results are a confirmation that, considering only simple concrete, carbonation can be beneficial, improving some of the properties of concrete. Measurements of porosity accessible to water (Table 6) show that carbonation makes concrete more compact, since 5% to 12% of the open porosity was closed. This can be one of the reasons, which explain the increase in mechanical strength.

Mercury intrusion curves of carbonated samples developed in a more irregular way and presented a total intrusion volume lower than those of control samples, indicating that the pore structures were really closed. The parameters used in this analysis (Table 7) were described in a previous work[18]. The open porosity of all are comparable, and the results of C40GC2A and C40GC2B, a little smaller than those of the others, are in agreement with the tendency already observed in the measurements of porosity accessible to water.

The pore surface area, threshold diameter, average and derived distribution diameter values in the end of the intrusion highlight the significant differences between the carbonated region (surface) and the non-carbonated region of the samples. The surface area of the pores is always larger

at the surface than inside the sample, even for the control sample, which may be due to the fact that the superficial regions are continually subject to interactions with the atmospheric elements, including natural carbonation of the control samples (originating from air contact). The threshold diameter, inflexion point of the intrusion curve (corresponding to the maximum in the dV/dD curve) of the carbonated samples is smaller than that of the control sample. Some authors[19,20] suggest that the threshold diameter corresponds to the smallest diameter of the pores, among the largest pores, which would constitute a percolation path into the sample. Therefore, the sharp decrease in the threshold diameter is an indicator of the closing of the pores as a result of carbonation. The average pore diameter (D_m) of the inner regions of the samples was practically the same, but the differences appear in the averages calculated for the surface regions, for which D_m is significantly smaller for the carbonated samples (about 60% smaller) as a result of the closing of the microstructure.

The carbonated samples present a pore structure more crooked than that of the reference sample. This conclusion, which already seemed to be indicated by the irregular intrusion curve, is confirmed by the significantly higher value of the retention factor (R), defined as being the ratio between the retained mercury volume after the first intrusion-extrusion cycle and the total volume of mercury introduced[18]. The slope of the tangent in relation to the intrusion curve near the point of maximum pressure (dV/dD in the end of the intrusion) indicates the existence of fine pores in the microstructure into which mercury did not succeed to enter and which must be identified and described by other techniques such as nitrogen adsorption, which was not used in this work. In conclusion, the smaller this slant, the smaller the existing fraction of fine pores. It can be noted from the values presented that the measures of this tangent obtained in the most superficial regions were always smaller than those of the inside of the sample, including of the reference sample (C40EC2), which would indicate a possible effect of the natural carbonation. However, the decrease in dV/dD in the end of the intrusion between the surface and the inside is much sharper for carbonated samples, reaching even the zero tangent for sample C40GC2, evidencing that carbonation promoted the closing of the fine pores to a large extent.

A last aspect, which must be considered in the analysis of mercury porosimetry results, is the morphology presented by the intrusion curves. Figure 2 reveals that the two curves related to the control sample (C40EC2) are practically overlapped, indicating that the pore size distribution coincides for the surface and the inside of the sample. Now, the carbonated samples present a much diverse behavior. Practically along all the distribution of the two samples analyzed, the superficial region, therefore which suffered carbonation, had always a mercury intrusion value lower than that of the inner region. In this way, carbonation seems to promote the closing of the pore structure in all the distribution of the sizes presented by the structure.

The microstructure observed in the concrete samples by SEM can be classified as compact, presenting few pores and few fissures. In general, the microstructure was uniform. In Fig. 3, some cement hydration products can be

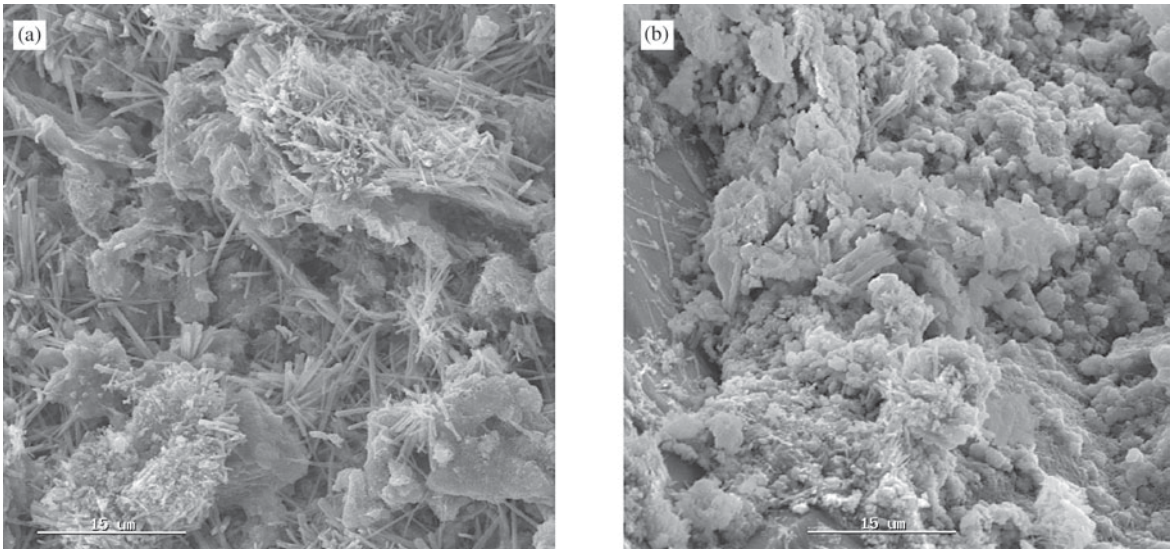

Figure 3. Photomicrographs of Concrete: a) region of formation of ettringite; b) portlandite and calcium silicates.

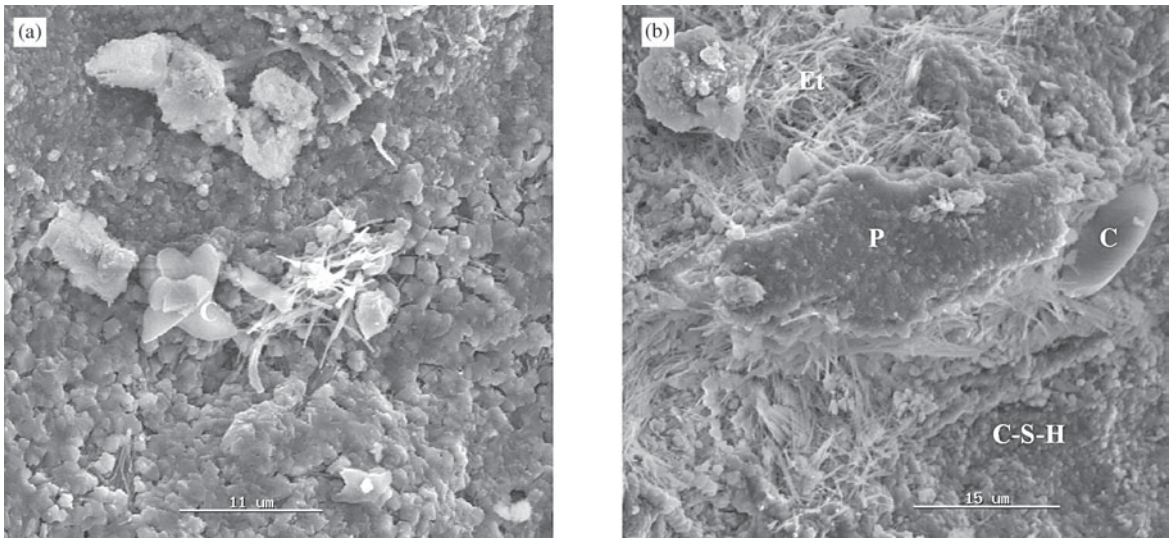

Figure 4. Photomicrographs of Concrete: a) presence of carbonates (C); b) several elements of the microstructure: carbonates (C), portlandite (P), calcium silicates (C-S-H) and ettringite (Et).

observed, such as some ettringite agglomerates (Fig. 3a) and C-S-H particles mixed with portlandite (Fig. 3b). Carbonates were also identified in some micrographs and are presented in Fig. 4.

6. Conclusions

The main conclusions of this work are summarized below:

1. The values of flexural strength obtained after the carbonation test show a decrease of 12% and 25% in relation to the values previously obtained on the 28th and 91st days, respectively. The carbonated concrete seems to present a decrease in its flexural strength.
2. The carbonated samples submitted to the compression test reached rupture with loads significantly higher (22 a 78%) than the control samples did.
3. Carbonation provoked a reduction of 5% to 12% of the open porosity of concrete.
4. The analysis of the results of the mercury porosimetry showed clearly the closing of the structure of the pores of the material as a result of the carbonation effect:
   a) The pore surface area is always larger in the surface than inside the sample, even for control samples;
   b) The threshold diameter of the carbonated samples is an order smaller than that of the control sample;
   c) The average diameter of pore distribution (D_m) of the superficial regions is significantly smaller in carbonated samples (about 60% smaller);
   d) The significantly higher value of the retention factor (R) of the carbonated samples seems to point to a pore structure more crooked than that of the reference sample, which already seemed indicated by the irregular intrusion curve;
   e) The slope (dV/dD) measurement in the end of the intrusion curve in the most superficial regions were always smaller than those inside the sample, including that of the reference sample (C40EC2), which would indicate for this sample a possible natural carbonation effect. However, the decrease in the value of dV/dD in the end of the intrusion between the surface and the inside is much sharper for carbonated samples, even reaching the zero tangent for sample C40GC2, demonstrating that the carbonation promoted the closing of a large part of these finer pores.
   f) Carbonation seems to promote the closing of the pore structure in all the size distribution presented by this structure.
5. The microstructure observed in the C40 concrete samples can be classified as compact, presenting few pores and fissures.

Acknowledgments

The authors thank FAPEMIG financial support.

References

1. Mehta, P.K. *In: Proceedings of II Intern. Conference on*

High-performance Concrete and..., Gramado, RS, p. 1-14, 1999.
2. Swamy, R.N. *In: Proceedings of Second CANMET/ACI Intern. Conference on High-performance Concrete*, ACI SP-186, p. 765-788, 1999.
3. DaSilva, T.J.; Roca, P. *In: Proceedings of Second CANMET/ACI Intern. Conference on High-performance Concrete*, ACI SP-186, p. 525-533, 1999.
4. Parrott, L.J. *Magazine of Concrete Research*, v. 46, n. 166, p.23-28, 1994.
5. Rigo da Silva, C.A.; Lemos, F.L.; Vasconcelos, W.L.; Lameiras, F.S. *In: 43ª Congresso Brasileiro de Cerâmica*, Florianópolis, SC, 1999.
6. Papadakis, V.G.; Vayenas, C.G.; Fardis, M.N. *ACI Materials Journal*, v. 88, n. 2, p. 186-196, 1991.
7. Mehta, P.K.; Monteiro, P.J.M. *Concreto: estrutura, propriedades e materiais*, Editora Pini, SP, Brasil, 581 p., 1994.
8. Neville, A.M. *Propriedades do Concreto*, Editora Pini, SP, Brasil, 828 p., 1998.
9. Rafai, N. *et al.*, *Cement and Concrete Research*, v. 21, n. 2/3, p. 368-377, 1991.
10. Kazmierczak, C.S.; Lindenmeyer, Z. *In: Proceedings of Intern. Congress on High-performance and...*, Florianópolis, SC, p. 402-413, 1996.
11. Papadakis, V.G.; Vayenas, C.G.; Fardis, M.N. *ACI Materials Journal*, v. 88, n. 4, p. 363-373, 1991.
12. Kobayashi, K.; Suzuki, K.; Uno, Y. *Cement and Concrete Research*, v. 24, n. 1, p. 55-61, 1994.
13. Deloy, F.X. *In: Proceedings of International Seminar*, Brasília, DF, p. 1-11, 1997.
14. Helene, P.R.L. *In: Proceedings of II Intern. Conference on High-performance Concrete and...*, Gramado, RS, p. 1-30, 1999.
15. Guimarães, A.T.C.; Dias, C.R.R.; Recena, F.A.P.; Helene, P.R.L. *In: Proceedings of II Intern. Conference on High-performance Concrete and...*, Gramado, RS, p. 1-18, 1999.
16. RILEM Commission 25 PEM, Test n. I.1 – Porosity accessible to water, *Matériaux et Construction*, RILEM, v. 13, n. 75, p. 177-179, 1980.
17. Rigo da Silva, C.A.; Reis, R.J.P.; Vasconcelos, W.L.; Lameiras, F.S. *In: Anais do V Encontro Nacional de Aplicações Nucleares*, Rio de Janeiro, RJ, p. 1-6, 2000.
18. Rigo da Silva, C.A.; Vasconcelos, W.L. *In: I Simpósio Brasileiro de Estruturologia*, Belo Horizonte, MG, p. 1-10, 1998.
19. Katz, A.J.; Thompson, A.H. *Physical Review B*, v. 34, n. 11, p. 8179-8181, 1986.
20. Halamickova, P. *et al.*, *Cement and Concrete Research*, v. 25, n. 4, p. 790-802, 1995.